Dysfunctional cilia lead to altered ependyma and choroid plexus function, and result in the formation of hydrocephalus

Boglarka Banizs[1], Martin M. Pike[2], C. Leigh Millican[3], William B. Ferguson[4], Peter Komlosi[4,5], James Sheetz[1], Phillip D. Bell[4,5], Erik M. Schwiebert[5,6] and Bradley K. Yoder[1,5,*]

[1]Department of Cell Biology, University of Alabama at Birmingham, Birmingham, AL 35294, USA
[2]Department of Medicine, Division of Cardiovascular Disease, University of Alabama at Birmingham, Birmingham, AL 35294, USA
[3]High Resolution Imaging Facility, University of Alabama at Birmingham, Birmingham, AL 35294, USA
[4]Department of Medicine, Division of Nephrology, University of Alabama at Birmingham, Birmingham, AL 35294, USA
[5]Nephrology Research and Training Center, University of Alabama at Birmingham, Birmingham, AL 35294, USA
[6]Department of Physiology and Biophysics, University of Alabama at Birmingham, Birmingham, AL 35294, USA
*Author for correspondence (e-mail: byoder@uab.edu)

Accepted 7 October 2005

Development 132, 5329-5339
Published by The Company of Biologists 2005
doi:10.1242/dev.02153

Summary

Cilia are complex organelles involved in sensory perception and fluid or cell movement. They are constructed through a highly conserved process called intraflagellar transport (IFT). Mutations in IFT genes, such as *Tg737*, result in severe developmental defects and disease. In the case of the *Tg737^{orpk}* mutants, these pathological alterations include cystic kidney disease, biliary and pancreatic duct abnormalities, skeletal patterning defects, and hydrocephalus. Here, we explore the connection between cilia dysfunction and the development of hydrocephalus by using the *Tg737^{orpk}* mutants. Our analysis indicates that cilia on cells of the brain ventricles of *Tg737^{orpk}* mutant mice are severely malformed. On the ependymal cells, these defects lead to disorganized beating and impaired cerebrospinal fluid (CSF) movement. However, the loss of the cilia beat and CSF flow is not the initiating factor, as the pathology is present prior to the development of motile cilia on these cells and CSF flow is not impaired at early stages of the disease. Rather, our results suggest that loss of cilia leads to altered function of the choroid plexus epithelum, as evidenced by elevated intracellular cAMP levels and increased chloride concentration in the CSF. These data suggest that cilia function is necessary for regulating ion transport and CSF production, as well as for CSF flow through the ventricles.

Key words: Cilia, Hydrocephalus, Tg737, Intraflagellar transport, Choroid plexus, Ependyma

Introduction

Hydrocephalus is a progressive pathological condition characterized by the excessive accumulation of cerebrospinal fluid (CSF) in the brain ventricles. It can be caused by impaired CSF flow, excess CSF production or a lack of CSF reabsorption, and it is one of the most common anomalies of the central nervous system (Bruni et al., 1985; Garton and Piatt, 2004). Current treatments involve surgical insertion of a ventricular shunt to facilitate drainage of excess CSF; however, shunt infections/malfunctions necessitate surgical revision in 15% of cases. Despite its high prevalence, in most cases of hydrocephalus the molecular mechanism(s) leading to the pathology remain elusive. Thus, in order to develop alternative treatment strategies, a better understanding of the pathogenesis of this disease is needed.

The CSF is produced largely by the choroid plexus (CP), a highly vascularized secretory neuroepithelium found in the lateral, third and fourth ventricles of the brain. These CP cells contain numerous microvilli associated with their highly secretory nature, and small tufts of cilia of unknown function (Doolin and Birge, 1966). The CSF is produced through the net directional transport of bicarbonate, chloride and sodium, with subsequent water movement through apical aquaporin 1 channels (Brown et al., 2004). The rates of CSF production and reabsorption must be in equilibrium; disturbances in the equilibrium lead to increased intracranial pressure and hydrocephalus.

The CSF circulates within the brain ventricles, from the lateral ventricle to the third ventricle, through the aqueduct of Sylvius into the fourth ventricle, and finally along the spinal channel and subarachnoid space where CSF is reabsorbed into the blood or lymphatic system (Weller et al., 1992). Although the mechanism(s) of CSF circulation remains poorly understood, one factor thought to have an important role is the orchestrated beating of cilia on the ependymal cells that line the ventricles and interventricular connections (Ibanez-Tallon et al., 2004).

Data from several studies suggest that impaired CSF flow generated by motile cilia on the ependyma results in aqueduct stenosis and a non-communicative form of hydrocephalus; however, it remains controversial whether the blockage of the duct is a primary cause or a consequence of compression exerted by the expanding ventricles (Ibanez-Tallon et al., 2004). In addition to the obstructive hydrocephalus, there are communicating forms where the duct remains patent. In this

form of hydrocephalus, the defect is thought to reside in excess CSF production by the CP or abnormal reabsorption by arachnoid villi (Britz et al., 1996).

Much of our understanding of hydrocephalus has come from the analysis of animal models. H-Tx rats develop congenital hydrocephalus. The mechanism leading to the pathology remains controversial: some studies indicate the primary defect is caused by duct obstruction, while others emphasize that the hydrocephalus develops prior to impaired CSF flow (Jones and Bucknall, 1988; Kiefer et al., 1998). Mice lacking the *E2f5* transcription factor exhibit communicating congenital hydrocephalus that has been attributed to the increased secretory activity of the CP; however, the role of *E2f5* in CSF production remains unknown (Lindeman et al., 1998). The hydrocephalus that develops in L1 neural adhesion molecule deficient mice, a molecule which is mutated in human forms of X-linked hydrocephalus, is initially associated with a patent aqueduct; however, duct stenosis occurs when the pathology becomes more severe (Rolf et al., 2001). There are also several mouse models of hydrocephalus that have been attributed to cilial dysfunction. Disruption of the outer dynein arm protein Mdnah5 (Dnahc5 – Mouse Genome Informatics) results in impaired cilia motility on ependymal cells. The subsequent loss of CSF flow is thought to contribute to aqueduct closure during early postnatal development, leading to hydrocephalus (Ibanez-Tallon et al., 2004). An analogous mechanism may be involved in the WIC-Hyd rats that also have impaired cilia motility (Torikata et al., 1991). In addition, mice with mutations in the cilia proteins Spag6 or hydin, or the transcription factor Hfh4 (Foxj1 – Mouse Genome Informatics) that lack ependymal cell cilia, all exhibit hydrocephalus (Chen et al., 1998; Davy and Robinson, 2003; Sapiro et al., 2002). Finally, cilia function in the CSF ventricular system is also important in humans, as evidenced by the incidence of hydrocephalus in human patients with primary ciliary dyskinesia (Bush, 2000). However, it should be noted that the effect of the cilia on the CP epithelium has not been evaluated in any of these models.

Another mouse model that develops hydrocephalus is the *Tg737*^{orpk} mutant. These mice exhibit hydrocephalus, cystic kidney disease, sterility, biliary and bile duct hyperplasia in the liver, acinar cell atrophy in the pancreas, retinal degeneration, and skeletal patterning abnormalities (Cano et al., 2004; Moyer et al., 1994; Taulman et al., 2001; Zhang et al., 2003; Zhang et al., 2005). The gene *Tg737* encodes a conserved protein called polaris that localizes to both motile and immotile cilia (Taulman et al., 2001). Analysis of polaris in mouse, as well as of its homologs in multiple organisms, indicates that its function is required for normal cilia formation. Polaris is a component of a large complex known as the Intraflagellar Transport (IFT) particle, which mediates the bidirectional movement of proteins from the base of cilia to the cilia tip (Haycraft et al., 2001; Pazour et al., 2000; Scholey, 2003). Here, we examine the connection between cilia defects and hydrocephalus in *Tg737*^{orpk} mutants, and evaluate the effects of cilial dysfunction on both ependymal and CP epithelium. As seen in *Mdnah5* mutants, the cilia defects on the ependymal cells in *Tg737*^{orpk} mice result in asynchronous beating and impaired fluid flow across the ependymal cell surface. However, our analysis indicates that abnormal cilial beating in *Tg737*^{orpk} mutants is unlikely to be the initiating factor, as hydrocephalus develops prior to the formation of motile cilia on the wild-type ventricular ependyma. In addition, the pathology is present in the absence of duct stenosis, indicating that blockage of CSF flow is also not the causative factor. Rather, our data support a model where cilia dysfunction leads to alterations in ion transport activity of the CP epithelia and, subsequently, to a marked increase in CSF production. Thus, we propose that the hydrocephalus in *Tg737*^{orpk} cilia mutants is not only a result of disrupted ependymal cilia-generated CSF flow, but is, primarily, the result of abnormalities involving cilia-regulated ion transport and CSF production by the CP.

Materials and methods

Mice

Tg737^{orpk} mice were generated as described previously (Moyer et al., 1994). The lines were maintained as heterozygous crosses on a FVB/N genetic background. Animals were treated and maintained in accordance with the IACUC regulations at the University of Alabama at Birmingham. Genotyping was performed as described previously (Yoder et al., 1997).

Morphological and histological analysis

Brains were fixed within the skull by removing the skull in the parietal region to allow formalin penetration into the tissue. Twenty-four-hour postfixation brains were removed and photographed. Fixed brains were then embedded into paraffin blocks and sectioned in coronal plane. Sections were stained with Hematoxylin and Eosin and photographed.

Magnetic resonance imaging (MRI)

Tg737^{orpk} mutant and wild-type littermates at postnatal day 1 and 6 were anesthetized using 1% isofluran. MRI was performed on a Bruker-Biospin 8.5T vertical wide-bore DRX-360 (UAB 8.5T Small Animal NMR Facility) with an AVANCE console, a Paravision 3.0.1 software platform, and a Mini0.5 imaging system equipped with a 56 mm inner diameter gradient set (Billirica, MA). Mice were positioned in a 20-mm birdcage resonator. Images were coronal T2 weighted RARE (8 echoes, rare factor 8) with the following parameters: TR 4.5 sec, effective TE 60ms, FOV 2.5 cm, 256×256 matrix, slice thickness 0.45 mm, in plane resolution 98 μm, four averages. The body temperature was maintained at 37°C. T2 RARE imaging allows detection of the fluid compartments without requiring the use of contrasting agents. Relative ventricular volume was calculated based on the intensity difference using ImageJ software (NIH).

Immunofluorescence microscopy

Mouse brains were isolated from wild-type and *Tg737*^{orpk} animals and processed for immunofluorescence microscopy as described previously (Taulman et al., 2001). Primary antibody dilutions were as follows: mouse anti-acetylated α-tubulin, 1:1500; rabbit anti-α-catenin, 1:500 (Sigma, St Louis, MI, USA); rabbit anti-polaris antibody, 1:500 (BY1700, Sigma-Genosys against amino acids LEIDEDDKYISPSDDPHTN); rabbit anti-polycystin-1 antibody, 1:300 (Ibraghimov-Beskrovnaya et al., 1997); and rat anti-zonula occludens, 1:40 (from Dr Daniel Balkovetz, UAB). Secondary antibodies conjugated to FITC and rhodamine Red-X were used at 1:500 (Jackson ImmunoResearch, West Grove, PA). Sections were analyzed by immunofluorescence using an inverted Nikon TE200 microscope and images were captured on a CoolSnap HQ/FX (Roper Scientific) CCD camera.

Proliferation analysis

Proliferation in CP cells from 3-day-old animals was determined by immunostaining with an anti-phospho-histone H3 antibody (diluted

1:300; Upstate, Lake Placid, NY). The proliferation index was assessed by counting the number of H3-positive cell nuclei per 1000 nuclei.

Scanning electron microscopy

Freshly isolated brains from wild-type and *Tg737*^{orpk} mutant animals were processed for scanning electron microscopy as described previously (Yoder et al., 2002). Samples were then analyzed on either ISI SX-40 or Hitachi 2460 Variable Pressure scanning electron microscopes.

Videorecording of ependymal cilia

The function of ependymal cilia was assessed as described previously (Ibanez-Tallon et al., 2004). Briefly, to capture beating of the ependymal cilia, fresh brain slices from either the lateral or fourth ventricle of 12-day-old animals were placed on a glass coverslip. Pre-warmed Phenol Red-free DMEM/F12 medium was mixed with a suspension of red fluorescent beads (50 μm, Sigma) and added to fresh brain slices. Cilia or particle movement was monitored by differential interference contrast (DIC) and fluorescence microscopy on a Nikon TE200 equipped with a CoolSnap HQ/FX CCD camera. Images were captured at 28 frames/second using MetaMorph software. The same program was used to track particle movement and to calculate mean speed of the tracked red fluorescent beads.

Brain ventricular injection of fluorescent DiI

Two- and 6-day-old animals were anesthetized using 100 mg/kg ketamine and 5 mg/kg xylazine, intraperitoneally. The right lateral ventricle was injected with 1.0 μl of 0.2% DiI using the following coordinates: depth 1.8 mm, lateral 0.9 mm crossing the line which bundle the posterior angles of orbitae bilaterally in 2-day-old mice, 0.8 mm posterior to this point in 6-day-old mice. Mice were then sacrificed and the brains were snap frozen and cryosectioned. Horizontal sections of injected brains were then fixed with 4% paraformaldehyde and nuclei stained with Hoescht. Sections were imaged using fluorescence microscopy. The time required for the dye to pass from the lateral ventricle into the fourth ventricle was determined by analyzing brain sections generated from mice 5, 10, 20 and 30 minutes post-injection.

Isolation of CSF

To isolate the CSF, 18- to 23-day-old wild-type or mutant animals were anesthetized as described above. CSF was harvested using a micromanipulator and a Hamilton syringe, with a 26-gauge needle with the following coordinates in mutant: Bregma –0.6 mm, lateral 1 mm, depth 1.8 mm. CSF was harvested from wild-type mice as described previously (DeMattos et al., 2002). Chloride ion concentration was determined with ion selective microelectrodes following the manufacturer's instructions (Lazarlabs, CA, USA).

Determination of $[cAMP]_i$ from isolated choroid plexus

Choroid plexi isolated from mutant and wild-type brains were immediately frozen in liquid nitrogen. Tissue processing and intracellular cyclic AMP content was determined using a competitive EIA assay system (Zymed Laboratories, CA, USA), following the manufacturer's instructions. Protein content was determined using DC Protein Assay Kit (BioRad Laboratories).

Statistical analyses

Values are means±s.e. Statistical significance was determined using an unpaired Student's *t*-test.

Results

Tg737^{orpk} mutant mice exhibit hydrocephalus

The *Tg737*^{orpk} hypomorphic mutant mice are severely growth retarded and normally die within the first few weeks of birth as a result of pathologies in multiple tissues, including hydrocephalus. The hydrocephalus phenotype in these mice is evident shortly after birth with an enlarged cranium. The gross appearance of the brain shows minor compression of the olfactory bulbs and cerebellum suggestive of increased intracranial pressure. Histological analysis indicates that the lateral ventricles are enlarged in mutants relative to the wild-type controls (Fig. 1).

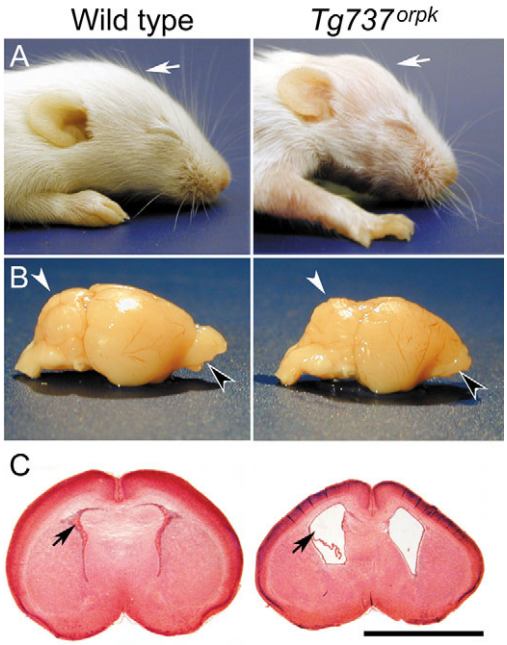

Fig. 1. *Tg737*^{orpk} mutant mice develop hydrocephalus. (A) Comparison of lateral views of 10-day-old wild-type and *Tg737*^{orpk} mice indicates that the mutants exhibit a bulging forehead (arrow), characteristic of hydrocephalus. (B) Gross analysis of the brains from mutants shows signs of compression at the olfactory bulb and the frontal pole of the cerebrum (black arrowhead). Also, the cerebellum is more prominent in mutant animals (white arrowhead) than in the wild-type control. (C) Hematoxylin and Eosin-stained coronal sections through identical regions of the brain demonstrate marked dilatation of the lateral ventricles (arrows) in mutant animals compared with wild-type controls. Scale bar: 4 mm.

Initiation and progression of the hydrocephalus in *Tg737*^{orpk} mutant mice

To follow the progression of hydrocephalus in vivo, we analyzed the phenotype of four pairs of mutant and wild-type littermates at postnatal day 1 and again at day 6 using T2 RARE magnetic resonance imaging (MRI). Coronal MRI sections of day 1 mutant brains exhibit larger fluid-filled lateral ventricles than those of their wild-type littermates (Fig. 2). Analysis of the same mutants at day 6 indicates that the lateral ventricles become even larger, whereas the wild-type lateral ventricles are small and difficult to distinguish from the surrounding brain tissue. The same results were seen from a paramedian sagittal view. Median-sagittal images were used to obtain information about the third ventricle-aqueduct-fourth ventricle axis, which is the narrowest portion of the entire ventricular system; its obstruction is the most frequent cause

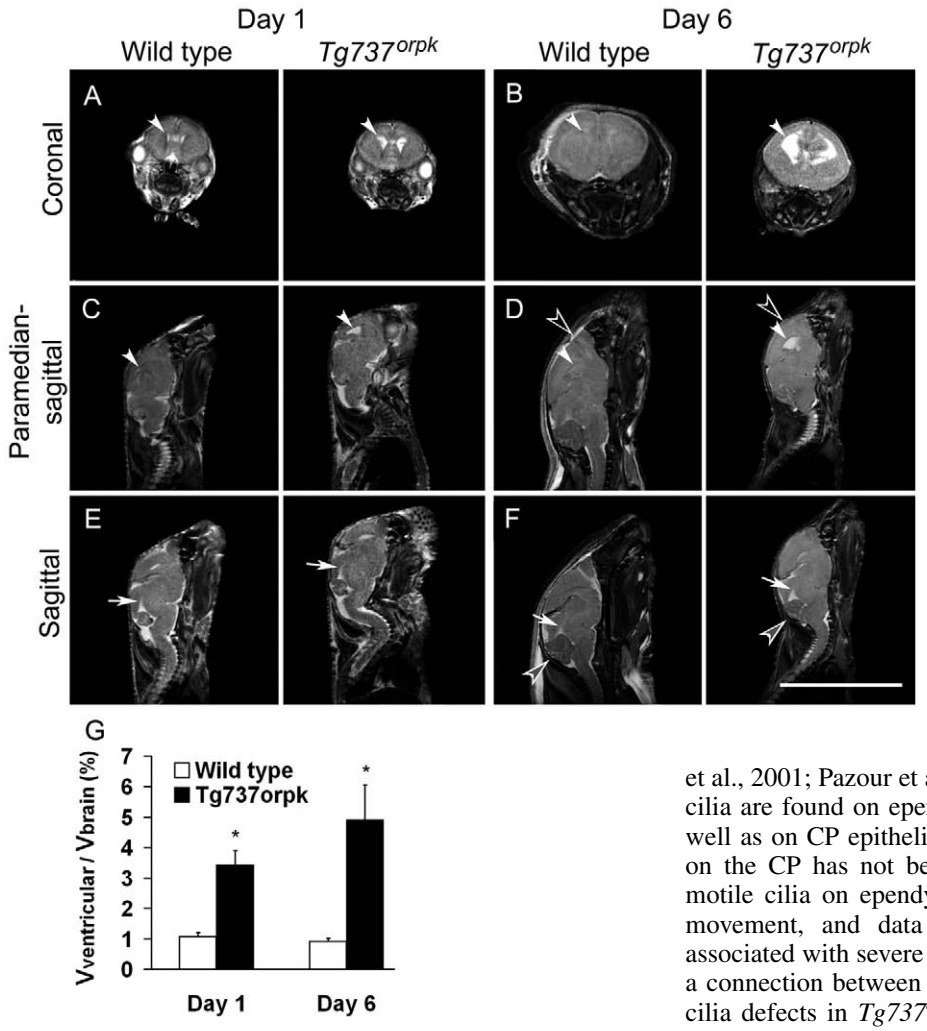

Fig. 2. Analysis of hydrocephalus progression in *Tg737*^{orpk} mutant mice using T2 RARE MRI. Compartments containing CSF appear white while brain matter is gray. (A,C) Dilatation is evident in the lateral ventricles (white arrowheads) of 1-day-old mutants as compared with wild types. (E) By contrast, there is no sign of expansion in the fourth ventricle or in the aqueduct (arrows) at this age. (B,D) By day 6, the lateral ventricles of the mutants are markedly enlarged (white arrowheads), without overt differences in the (F) fourth ventricle and aqueduct, but protuberance is seen on the skull above the cerebellum (gray arrowheads). (D) In the subarachnoid space, no difference is detected between wild-type and mutant animals (black arrowheads). Scale bar: 10 mm. (G) Quantitative measurement of the relative ventricular volume in mutant and wild-type controls at each age (n=4; *P<0.05).

of hydrocephalus. Median-sagittal sections of 1-day-old wild-type and mutant littermates reveal no overt morphological difference in this axis. By day 6, the protrusion of the cerebellum into the cisterna magna and the skull protuberance above the cerebellum indicate that increased intracranial pressure may be present in these animals, suggestive of duct obstruction. However, resolution of the MRI images was not sufficient to establish whether the aqueduct in the mutants was open or obstructed at these stages. Therefore, this was further addressed by the intra-ventricular injection of DiI (see below). The analysis of the MRI images indicated that the normalized ventricular volume was 3.1-fold and 5.3-fold higher in mutants than in wild-type controls at day 1 and 6, respectively. Thus, by day 1 there was already a significant increase in the ventricular volume.

In contrast to the ventricular data, MRI analysis did not show alterations in the subarachnoid space, suggesting that there are no overt defects in CSF reabsorption (Ruiz et al., 2004).

Cilia are malformed on *Tg737*^{orpk} mutant ependymal and choroid plexus epithelia

Previous data indicated that polaris and its homologs in *Chlamydomonas* (IFT88) and *C. elegans* (OSM-5) function as an IFT particle protein required for cilia formation (Haycraft et al., 2001; Pazour et al., 2000). Inside the ventricular system, cilia are found on ependymal cells that line the ventricles, as well as on CP epithelia. Although the importance of the cilia on the CP has not been explored, beating of the numerous motile cilia on ependymal cells is thought to facilitate CSF movement, and data indicate that loss of these cilia is associated with severe hydrocephalus. Thus, to further explore a connection between the pathogenesis of hydrocephalus and cilia defects in *Tg737*^{orpk} mutants, we compared the cilia on the ependyma and CP epithelia in mutant and wild-type mice by immunofluorescence and by scanning electron microscopy.

The ependymal cells of adult mice have numerous long cilia that extend into the ventricular lumen. On wild-type CP epithelium, most cells have a small tuft of cilia on the apical surface; however, there are also numerous CP cells with a single primary cilium. The functional importance of these cilia types is unknown (Fig. 3).

In agreement with the hypomorphic nature of the *Tg737*^{orpk} mutation, polaris expression and cilia were still detected on the ependyma and CP epithelium of mutant animals. Compared with wild-type controls, the cilia on the mutant ependyma were fewer in number, disorganized, stunted and anisometric, and often exhibited a bulb-like structure at their tips in which the mutant form of the polaris protein accumulated (Fig. 3). These bulb-like structures were also observed on the CP epithelia and, as seen on the ependyma, the mutant form of polaris was concentrated at the tip. These morphological differences were also evident using scanning electron microscopy and are in agreement with recently published data showing that primary cilia on renal collecting duct cells of *Tg737*^{orpk} mutants also have this bulb-like structure (Liu et al., 2005).

Malformed cilia in *Tg737*^{orpk} mutants result in impaired beat and reduced fluid flow

The cilia morphology defects on the ependymal cells of

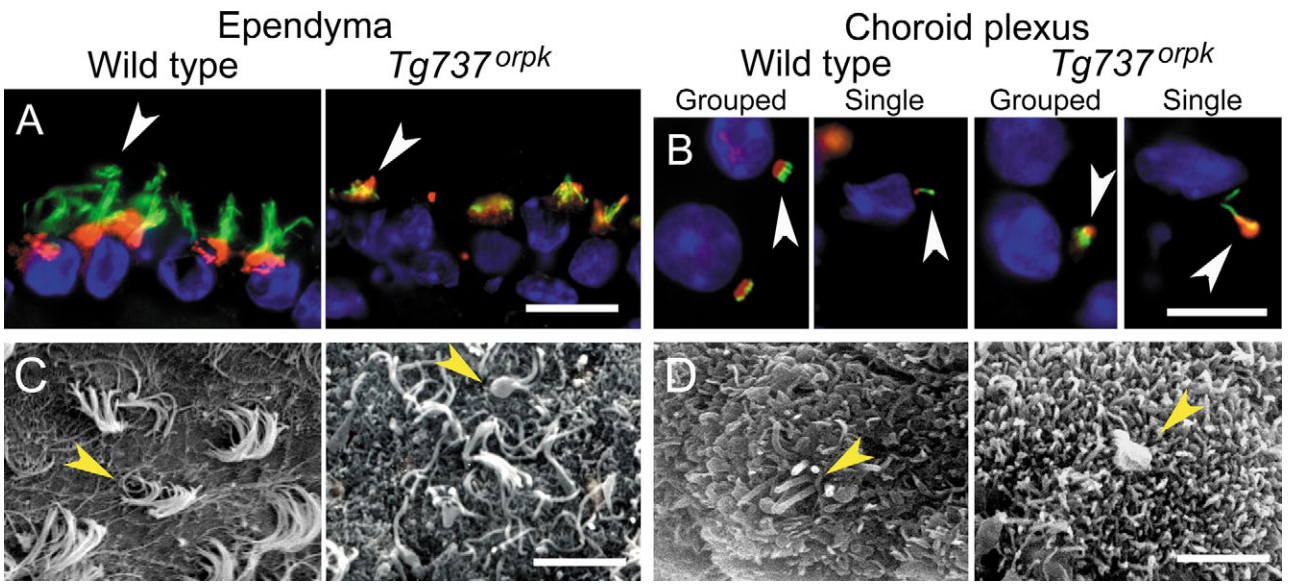

Fig. 3. Altered cilia morphology on cells of the ventricular system in *Tg737*^{orpk} mutant mice. Photomicrographs of brain sections from wild-type and mutant animals, showing immunolocalization of acetylated-α-tubulin (green) and polaris (red). White and yellow arrowheads indicate cilia. (A) Ependymal cilia in wild-type mice are in well-organized groups, with equal length, whereas cilia on the *Tg737*^{orpk} mutant ependyma are fewer in number, shorter and anisometric. Polaris predominantly localizes to the basal body in the wild-type ependyma, but is found to accumulate at the cilia tip in the mutants. (B) Grouped and primary cilia are present on the CP of wild-type mice and polaris is concentrated at the basal bodies. Polaris accumulates at the tip of the grouped and primary cilia in *Tg737*^{orpk} mice. Cilia often exhibit a large bulb-like structure in which polaris is concentrated. (C) Scanning electron microscopy of ependymal cilia of normal and *Tg737*^{orpk} mutant mice. (D) Cilia on the CP of normal and *Tg737*^{orpk} mutants. In mutants, the cilia are morphologically abnormal with a thickened axoneme. Scale bars: in A, 20 μm; in B, 10 μm; in C, 15 μm; in D 2.5 μm.

Tg737^{orpk} mutants suggest that hydrocephalus may be associated with an altered cilia beat and, subsequently, impaired CSF movement. To assess these possibilities, we analyzed cilia beating on freshly isolated ependymal cells using time-lapse DIC and fluorescence microscopy with small fluorescent beads added to track fluid movement (see Movie 1 in the supplementary material). On wild-type ependyma, cilia beat was rapid, well orchestrated, and produced a laminar flow across the cells. By contrast, the movement of cilia on mutant ependyma exhibited a low frequency beat, which was asynchronous and failed to produce a significant amount of directional fluid flow (Fig. 4). Thus, as seen for other mouse mutants, the defect in cilia motility in the *Tg737*^{orpk} mutants is consistent with the impaired CSF flow through the ventricles and with the development of hydrocephalus (Ibanez-Tallon et al., 2004).

The hydrocephalus in *Tg737*^{orpk} mutants precedes the formation of motile cilia on ependymal cells

To further evaluate a connection between cilia defects, impaired CSF flow and the etiology of hydrocephalus, we analyzed when and where motile cilia first become evident on cells in the ventricular system of wild-type mice, and correlated these data with the appearance of hydrocephalus in the *Tg737*^{orpk} mutants.

Our analysis of cilia formation on ependymal cells using serial-section immunofluorescence indicated that, in one-day-old wild-type mice, most ependymal cells lining the ventricles had only a primary cilium. The presence of the multi-ciliated cells did not occur on the ventricular walls until around postnatal day 7. This was well after the pathology develops in the *Tg737*^{orpk} mutants (postnatal day 1), suggesting that the loss of these motile cilia and the subsequent flow generated by them cannot be the cause of the hydrocephalus. One exception to this was the cells lining the aqueduct interconnecting the third and fourth ventricle. Most of these cells were multi-ciliated by postnatal day one (Fig. 5). Thus, the loss of motile cilia in the aqueduct of mutants could impair flow through the duct and lead to a pathology similar to obstructive hydrocephalus.

In contrast to the ependymal cells, the cilia on wild-type CP epithelium were well formed by day 1 and were similar to those seen in the adults. Because these cilia are present when the hydrocephalus initiates, loss of their function could contribute to the pathology. Although cilia on the multi-ciliated CP epithelium are motile (data not shown), our analyses indicate that they would have a minimal effect on generating CSF flow.

Initiation of hydrocephalus in *Tg737*^{orpk} mice occurs prior to aqueduct stenosis

In contrast to the ependymal cells lining the ventricular walls, motile cilia were present on aqueduct cells prior to the onset of hydrocephalus, raising the possibility that an impaired function of these cilia may initiate the phenotype. This could occur by duct stenosis, which is normally inhibited by the beating of the cilia on these cells, or by impaired CSF flow through these narrow structures in the absence of normal cilia beat.

To begin testing these possibilities, CSF flow was evaluated

by using the fluorescent dye DiI injected into one lateral ventricle of 2- and 6-day-old wild-type and *Tg737*^{orpk} mutant mice. The movement of DiI through the ventricles was analyzed by serial sectioning of the brain. To initiate this analysis, we evaluated DiI movement in wild-type (day 2 and 6) mice at 5, 10, 20, and 30 minutes after injection into the lateral ventricle to determine the time needed for it to be detected in the fourth ventricle. DiI was detected at all time points except for at 5 minutes, thus all subsequent analyses were performed after 10 minutes (Fig. 6). Our analysis of 2-day-old mutants was indistinguishable from that of the wild-type controls. This confirms that the aqueduct remains patent in the early stages of the disease and that the impaired motility of the cilia lining the aqueduct at this early age does not result in an obstructed CSF flow that could cause the pathology. In contrast to the 2-day-old mutants, in 6-day-old *Tg737*^{orpk} mice, DiI was not detected in the fourth ventricle, indicating that passage through the aqueduct had been compromised. Because this occurs late in the pathogenesis of the disease in these mutants, the duct stenosis and loss of flow is likely to be a consequence, rather than a cause, of the hydrocephalus.

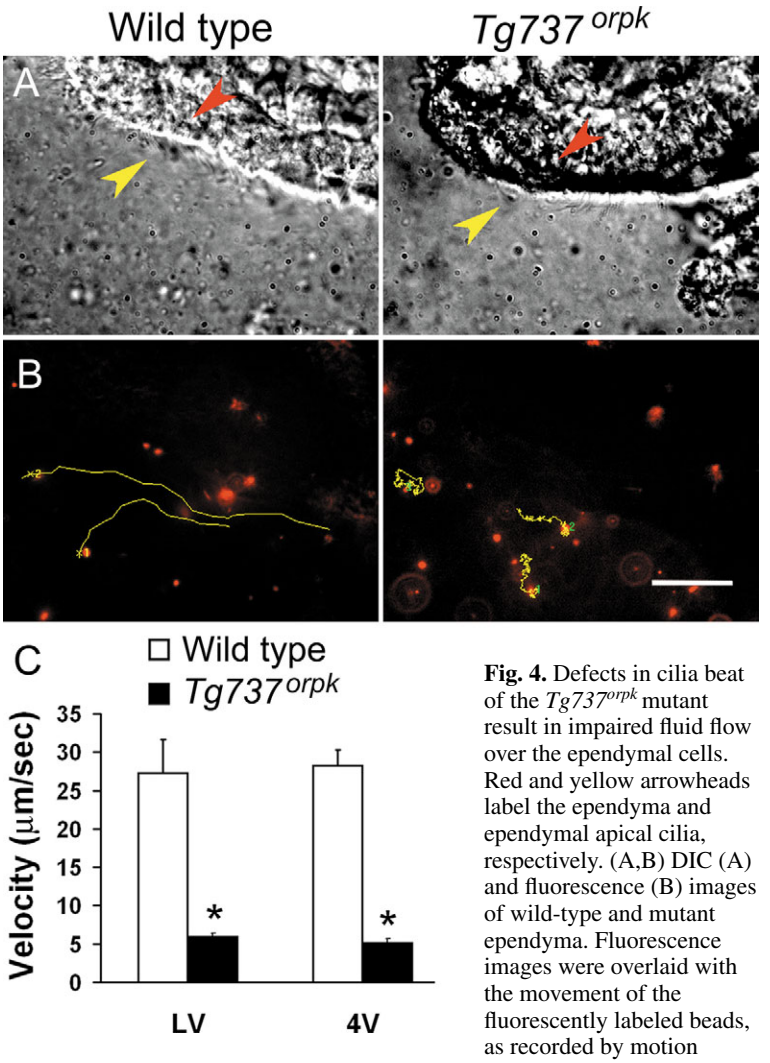

Fig. 4. Defects in cilia beat of the *Tg737*^{orpk} mutant result in impaired fluid flow over the ependymal cells. Red and yellow arrowheads label the ependyma and ependymal apical cilia, respectively. (A,B) DIC (A) and fluorescence (B) images of wild-type and mutant ependyma. Fluorescence images were overlaid with the movement of the fluorescently labeled beads, as recorded by motion tracking (yellow lines, see Movie 1 in the supplementary material). Movement of the beads propelled by wild-type cilia beating was rapid and directional, whereas movement of the beads in the mutant samples was random. Scale bar: 20 μm. (C) Graph showing quantitative analysis of the flow generated by the cilia in the left (LV) and fourth (4V) ventricles from mutant and wild-type samples (n=6; *P<0.005).

Cell polarity on the choroid plexus epithelia of *Tg737*^{orpk} mutants

Another potential pathogenic mechanism is altered cell polarity, similar to that seen for the kidneys of *Tg737*^{orpk} mice, as well as of several other PKD mouse models, which have revealed a mislocalization of polarized proteins such as the EGF receptor and Na^+/K^+-ATPase (Wilson, 1997). In the kidney, this results in excess fluid accumulation in the tubules and the development of the cystic pathology (Avner, 1993; Wilson, 1997). Here, we analyzed sections of brains to determine the localization of α-catenin and ZO-1 (Tjp1 – Mouse Genome Informatics), indicators of general polarity as well as of transport proteins such as the Na^+/K^+-ATPase and the anion exchanger 2 (Fig. 7). The data indicate that all of these proteins were localized normally in the mutants and at similar levels to in the control samples. Thus, there were no overt defects in the organization of the tissue because of defects of the cilia.

Another aspect of polarity that we analyzed was whether the distribution of signaling proteins in the cilia axoneme was affected. An altered localization of proteins in the axoneme could lead to their dysfunction and impair the sensory or signaling activity of these cilia, as has been proposed to occur in the kidneys of cystic mutants (Olteanu et al., 2005; Liu et al., 2005). Because there are no data with regards to signaling proteins in the cilia of the CP, on the basis of previous studies of renal cilia, we evaluated whether polycystin-1 (Pkd1 – Mouse Genome Informatics) was present in the cilia of the CP and whether its distribution was affected by the *Tg737* mutation. Polycystin-1 is an integral cilia membrane protein involved in a fluid flow-induced calcium signaling pathway (Nauli et al., 2003; Praetorius and Spring, 2003). As seen in primary cilia of the kidney, polycystin-1 localized predominantly at the basal bodies in both multi- and primary ciliated cells and at lower levels along the cilia axoneme in wild-type CP (Fig. 8). By contrast, in *Tg737*^{orpk} mutants, polycystin-1 was concentrated in the bulb-like structure at the tip of cilia in CP, rather than in the basal body (Fig. 8). Although polycystin-1 mutations are not associated with hydrocephalus, this example supports the possibility that there may be cilia-mediated signaling defects in the CP of the *Tg737*^{orpk} mutants resulting from the mislocalization of cilia proteins in the axoneme, which may result in the subsequent transmission of a signal from the cilia into the cell, as has been proposed for cystic kidney disease (Sutters and Germino, 2003).

Analysis of proliferation in the choroid plexus epithelium of *Tg737*^{orpk} mutants

There are several models of hydrocephalus where pathogenesis

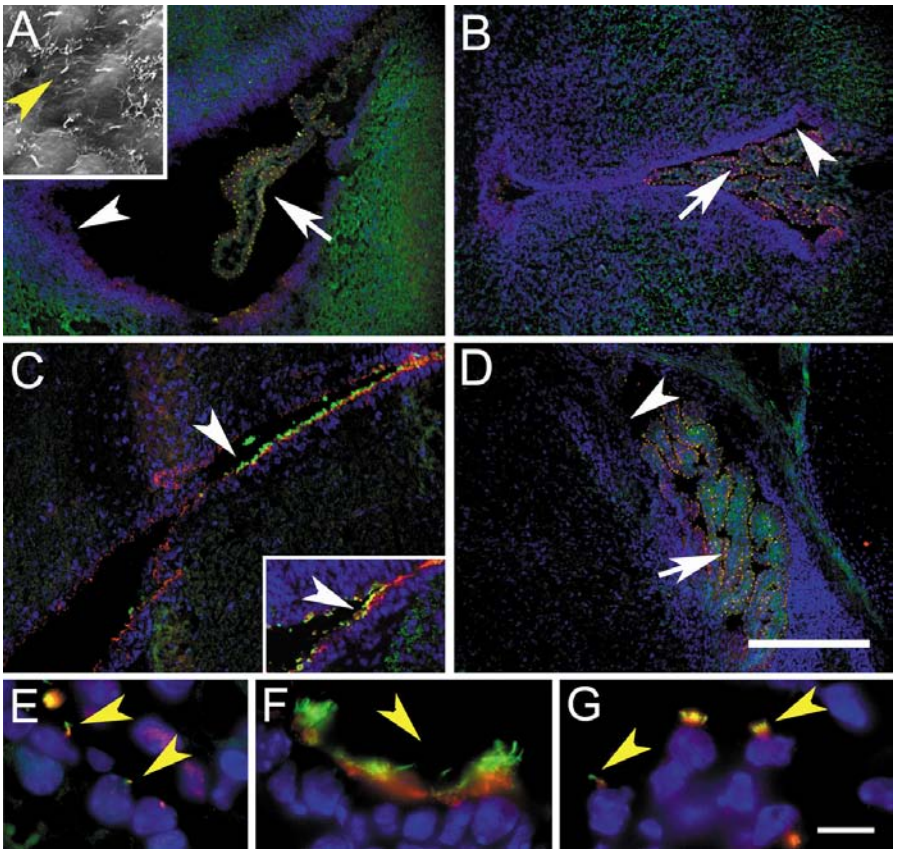

Fig. 5. Analysis of cilia in the ventricular system in 1-day-old mice. Brain sections of a 1-day-old wild-type mouse containing the (A) lateral and (B) third ventricles, (C) the aqueduct and (D) the fourth ventricle were analyzed for the presence of cilia (anti-acetylated-tubulin, green; polaris, red) on the ependyma (white arrowheads) and the choroid plexus epithelia (white arrow). No multi-ciliated cells were evident on the ependyma of the (A) lateral, (B) third or (D) fourth ventricles at this age. Ependymal cells possess primary cilium, as shown by the SEM and immunofluorescence (inset in A,E; yellow arrowheads). (C) By contrast, the ependymal lining of the aqueduct was multi-ciliated (white arrowhead). Inset shows that multiple cilia are also present in the mutant aqueduct. (F) Multiple cilia cover cells in the aqueduct (yellow arrowheads). (G) Grouped and single cilia on the choroid plexus. Scale bars: in A-D, 200 μm; in E-G, 10 μm.

is associated with excess CSF production due to the hyperproliferation of CP cells (i.e. CP papillomas). In addition, a hallmark of cystic kidney disease is increased proliferation of the cystic epithelium. To determine whether increased CP cell number is associated with the pathology, we evaluated whether proliferation was altered in the CP of *Tg737*^{orpk} mutants. The data indicate that there are no significant differences in proliferation in the CP between wild type and the *Tg737*^{orpk} mutants (Table 1).

Tg737^{orpk} mutants have increased intracellular cAMP levels in the choroid plexus and an elevated chloride concentration in the CSF

An alternative mechanism associated

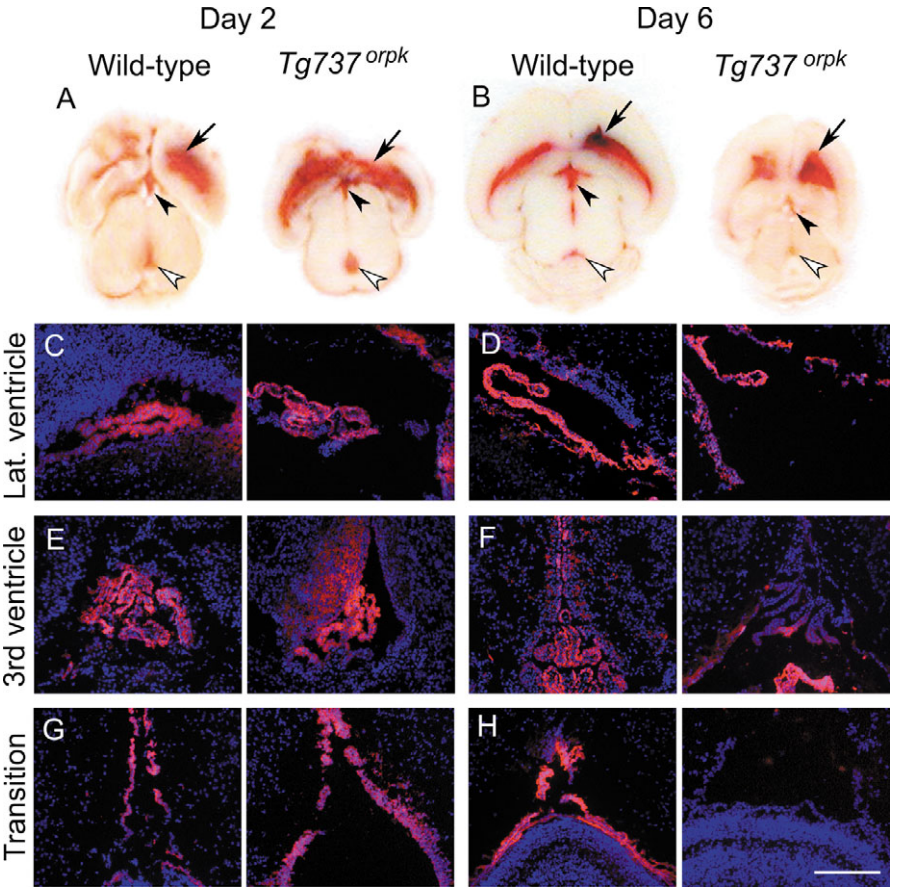

Fig. 6. The initiation of hydrocephalus precedes aqueduct stenosis in *Tg737*^{orpk} mutant mice. Movement of DiI (red) was tracked through brain sections of 2- and 6-day-old wild-type and *Tg737*^{orpk} mutant mice, 10 minutes post-injection. (A,B) Horizontal view of brains showing the lateral ventricles (black arrows), third ventricle (black arrowheads) and fourth ventricle (white arrowheads). (C-H) Fluorescence images of brain sections through the indicated regions from (C,E,G) 2-day-old and (D,F,H) 6-day-old control and mutant mice. DiI is detectable in the fourth ventricle of 2-day-old mutants (A,G, right panels), but is not seen in 6-day-old mutants (B,H, right panels), indicating that CSF movement was obstructed in these mutants. Scale bar: 200 μm.

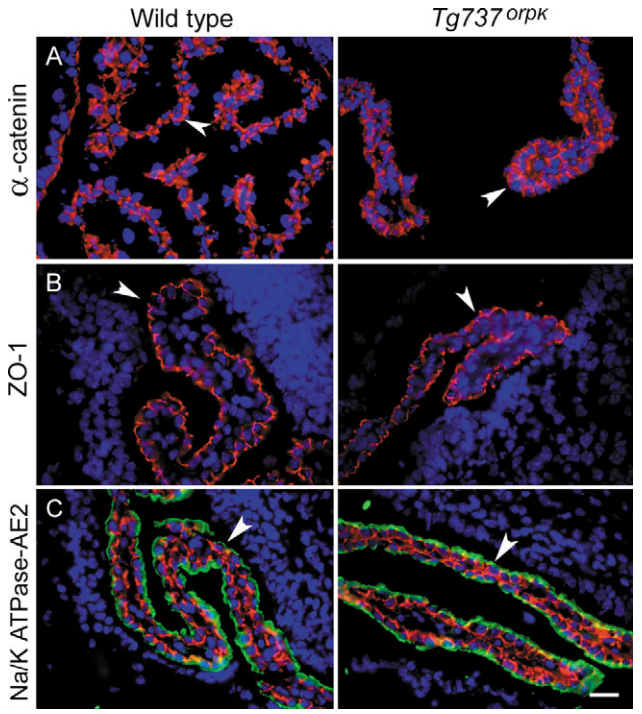

Fig. 7. *Tg737*^{orpk} mutant mice demonstrate no overt loss of epithelial polarity in the choroid plexus. Arrowheads indicate the apical surface of the choroid plexus. (A) Expression of α-catenin (red) in sections of wild-type and mutant mice. (B) ZO-1 (red) is localized to the tight junctional complexes near the apical surface of wild-type and mutant choroid epithelia. (C) Analysis of transport proteins Na^+/K^+ATPase (green) and the anion exchanger type 2 (AE2, red) shows normal localization at the apical and basolateral membranes, respectively. Scale bar: 20 μm.

with the development of hydrocephalus could be elevated CSF production. Nearly all CSF is produced by the CP through the directional transport of chloride and bicarbonate to the ventricular lumen (apical) (Brown et al., 2004). Thus, to determine whether cilia dysfunction may have an effect on CSF production, we compared chloride concentration in CSF isolated from mutant and wild-type mice. The chloride level was significantly higher in mutant CSF relative to the wild-type controls (Fig. 9).

Chloride transport into the CSF is regulated in part by an apically localized inward-rectifying chloride channel, which is activated by intracellular cyclic AMP (cAMP) signaling (Brown et al., 2004; Kibble et al., 1997). To investigate a possible mechanism leading to the elevated chloride level in mutant CSF, we measured the intracellular concentrations of

Table 1. Cell proliferation in the CP of *Tg737*^{orpk} mutant mice

Mice	Proliferation index (positive nuclei/nuclei)
Wild type	$(3.75\pm0.31)\times10^{-3}$
Tg737^{orpk} mutant	$(4.175\pm0.36)\times10^{-3}$, n.s.

Comparison of mean±s.e. values for positive cells (positive nuclei/nuclei) of mutant and wild-type mice (n=5).
n.s., not significantly different from wild-type control.

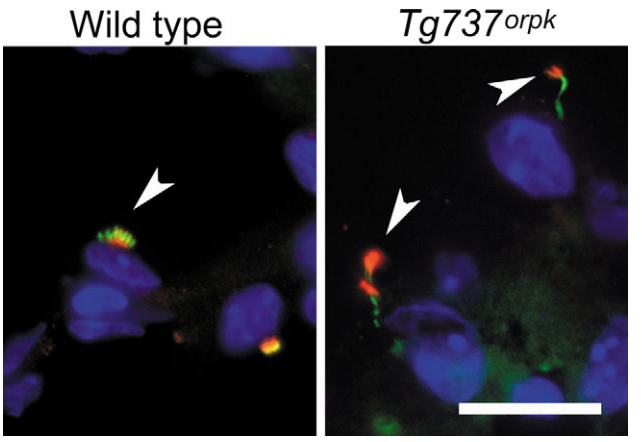

Fig. 8. Altered localization of proteins in the cilial axoneme of *Tg737*^{orpk} mutants. On the wild-type choroid plexus, polycystin 1 (red) was localized predominantly at the base of the cilia (acetylated-α-tubulin, green), whereas, in the mutants, polycystin 1 accumulated in the bulb-like structures at the cilia tip. Scale bar: 20 μm.

cAMP in CP cells freshly isolated from 5-day-old mutant and wild-type mice. In support for elevated chloride secretion by the CP, the intracellular levels of cAMP were significantly increased in mutant animals when compared with the wild type (Fig. 9).

Together, these data suggest that the loss of normal cilia function on the CP results in aberrant cAMP-regulated chloride transport, which would lead to enhanced fluid movement into the ventricle lumen and to excess CSF production.

Discussion

Hydrocephalus is a relatively common birth defect (Bruni et al., 1985; Garton and Piatt, 2004). Despite the prevalence of this disorder, and the existence of several genetic and induced models of the disease in mice and rats, our understanding of the molecular and cellular mechanisms causing the pathology has remained largely enigmatic. The proposed causes of hydrocephalus vary, but they are all center on the net accumulation of CSF resulting from CSF overproduction, blocked CSF flow or impaired CSF reabsorption. Due to our limited understanding of the causative mechanisms, current

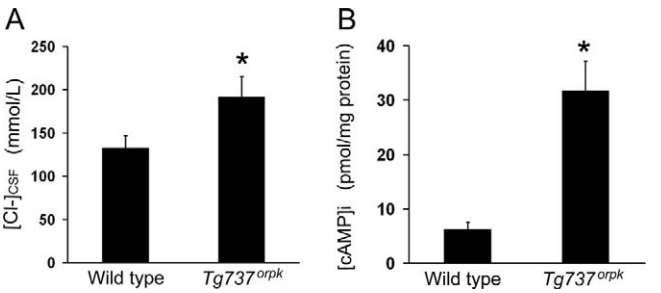

Fig. 9. Choroid plexus physiology is altered in the *Tg737*^{orpk} mutants. Graphs indicating (A) the chloride concentration in the CSF of wild-type and mutant mice, and (B) the intracellular cyclic AMP level ($[cAMP]_i$) in the CP epithelium from wild-type and mutant animals (n=6 and n=7, respectively; A, *P<0.05; B, *P<0.005).

treatment strategies are palliative and rely on the insertion of shunts to drain excess CSF, and reduce intracranial pressure and subsequent ventricular expansion.

We utilized *Tg737*^{orpk} hypomorphic mutants to further explore the connection between cilia and the development of hydrocephalus. MRI and histological analysis of *Tg737*^{orpk} mutants indicated that the pathology is progressive and that it can be detected in the perinatal period. Because polaris is required for cilia assembly (Haycraft et al., 2001), we initially suspected that the hydrocephalus in *Tg737*^{orpk} mutants would be associated with a loss of motile cilia and a subsequent impaired CSF flow, as has been shown for other hydrocephalus mouse models (Ibanez-Tallon et al., 2004; Torikata et al., 1991). Indeed, our analysis of the cilia in *Tg737*^{orpk} mutants shows severe morphological abnormalities on the ependymal cells. This is similar to the pathogenic mechanism reported for the *Mdnah5* axonemal dynein mutant. In *Mdnah5* mutants, cilia on ependymal cells form normally but are paralyzed and result in an impaired CSF flow. This lack of CSF movement is thought to be an initiating factor leading to increased intracranial pressure, duct stenosis and the development of hydrocephalus, which becomes evident after postnatal day 6 (Ibanez-Tallon et al., 2004).

In support of an impaired CSF flow mechanism, our in vitro analysis of the ciliary beat and fluid flow generated by the cilia on the ependymal cells isolated from the lateral ventricle of *Tg737*^{orpk} mutants revealed that the beat is disorganized and flow is impaired. However, when we correlated the time at which the pathology becomes evident (postnatal day 1) in the *Tg737*^{orpk} mutants with when the motile cilia actually form on cells in the ventricles, the data do not support a direct role for impaired cilia beat as being an initiating factor. An exception to this was the cells that line the aqueduct interconnecting the third and fourth ventricles. Unlike the ependyma lining the ventricles, this ductal epithelium possesses motile cilia that are present prior to onset of the pathology. However, our in vivo analyses of CSF movement using DiI injection indicate no differences in CSF flow between the mutant and wild-type controls at early stages of the disease. Impaired CSF movement was evident only after significant expansion of the ventricles, suggesting that loss of CSF flow is a consequence of the pathology. These data raise the possibility that a mechanism other than duct obstruction or loss of CSF flow is the initiating factor leading to the development of hydrocephalus.

Another possible mechanism involves defects in the CP. The CP is a specialized secretory organ located within the brain ventricles, and its primary functions are the production and homeostasis of the CSF (Strazielle and Ghersi-Egea, 2000). Our analyses of the CP cells indicate that there are two populations, one that has small tufts of motile cilia and another that has a single primary cilium. The function(s) of either of these types of cilia on the CP has not been explored. To our knowledge, this is the first description of primary cilia on the CP, and we speculate that these cilia have sensory roles similar to that shown in the embryonic node and in the renal tubules.

Although not as common as obstructive hydrocephalus, where CSF movement is impaired, communicative forms of this disease have also been described that result either from a delayed reabsorption by arachnoid granulae or an excess CSF accumulation, such as in the case of CP tumors. In most cases where there are defects in reabsorption, MRI analysis reveals an expansion in the subarachnoid space. This is not evident in the *Tg737*^{orpk} mutants, which suggests that impaired reabsorption is not the cause. As there is no overgrowth or increased proliferation of the CP in *Tg737*^{oprk} mutants, any effects on CP function would likely occur at the level of a pathway regulating the secretory behavior of these cells. Thus, it is intriguing that our analysis of CSF composition indicates a significant increase in the level of chloride. Chloride is transported through the activity of an unidentified, apically localized, inwardly rectifying chloride channel that is regulated by cAMP. Thus, the increased chloride level in the CSF is supported by the elevated intracellular cAMP concentration in the CP epithelium. The elevated chloride level in the CSF suggests that the altered ion transport properties of the CP result in an increased fluid movement and an excess CSF production that would contribute to the development of hydrocephalus. The physiology causing this increased chloride transport and the connection to cilial function is currently under investigation.

Intriguingly, in the *E2f5* mutants, defects in CP secretory behavior are thought to cause a communicating form of hydrocephalus, as seen in early *Tg737*^{orpk} mutants (Lindeman et al., 1998). This may be analogous to the mechanism of renal cyst development in mice and humans with cilia dysfunction (Guay-Woodford, 2003). Several studies have shown that elevated cAMP signaling caused by the vasopressin receptor type 2 results in excess fluid secretion across cystic epithelium, the inhibition of which abrogates the cystic pathology. Thus, it will be interesting to evaluate whether a similar mechanism is involved in the hydrocephalus pathology in *Tg737*^{orpk} mice (Sullivan et al., 1998; Torres, 2004).

Overall, the brain pathology in the *Tg737*^{orpk} mutants appears to be a consequence of several cilia dysfunction-mediated events. The first, which we believe is an initiating factor, involves altered ion transport across the CP epithelium and an increase in the production of CSF. How impaired cilia or polaris function in the CP epithelium affects the localization, expression or activity of proteins involved in ion movement, and which proteins are specifically involved, is being evaluated. One possibility is that the loss of normal polaris function in the mutants results in an altered distribution of a transporter/channel/exchanger in the cilia axoneme, which, subsequently, leads to their aberrant function. The precedent for this has been established by the case of polycystin 1. Polycystin 1 is required for the flow-induced calcium signaling mediated by the deflection of the primary cilium on renal epithelium, and, recently, it has been shown that this flow-induced calcium signal is similarly abrogated in perfused tubules from *Tg737*^{orpk} mutants (Liu et al., 2005). Thus, we expect that the loss of, or deformed, cilia on cells of the CP may alter the function of proteins involved in ion transport and CSF production, similar to that which occurs in the renal epithelia of cystic kidney diseases. It is interesting to speculate that similar defects might occur in the epithelia of other tissues (i.e. the biliary duct and pancreatic duct) affected in the *Tg737*^{orpk} mutants. Thus, understanding how cilia organize directional ion transport and CSF production in the CP may provide important insights into the pathogenesis of several other diseases involving cilia dysfunction.

The second event is likely to be the loss of cilia beat on the ependymal cells lining the ducts and ventricles. Previous studies in mice, such as in the *Mdnah5* mutant, indicate that

motile cilia do have important roles in CSF movement and that the loss of these motile cilia leads to hydrocephalus. Based on our analysis of when and where motile cilia form in relation to disease pathogenesis in the *Tg737*^{orpk} mutants, it is likely that the progression of the disease is exacerbated by the impaired CSF movement through the ducts connecting the ventricles. This would result in increased intracranial pressure, ventricular expansion and duct stenosis, with rapid progression of the disease.

We thank Dr Katherine Klinger (Genzyme, Framingham, MA, USA) for providing polyclonal anti-polycystin-1 antibody; members of Yoder laboratory for their discussion on the manuscript; and Paul Blanchard (Samford University, Birmingham, AL, USA) for helping us with SEM. This work was supported, in part, by NIH grants to B.K.Y. (RO1 DK65655 and RO1 DK62758).

Supplementary material

Supplementary material for this article is available at
http://dev.biologists.org/cgi/content/full/132/23/5329/DC1

References

Avner, E. D. (1993). Epithelial polarity and differentiation in polycystic kidney disease. *J. Cell Sci.* **17**, 217-222.

Britz, G. W., Kim, D. K. and Loeser, J. D. (1996). Hydrocephalus secondary to diffuse villous hyperplasia of the choroid plexus. Case report and review of the literature. *J. Neurosurg.* **85**, 689-691.

Brown, P. D., Davies, S. L., Speake, T. and Millar, I. D. (2004). Molecular mechanisms of cerebrospinal fluid production. *Neuroscience* **129**, 957-970.

Bruni, J. E., Del Bigio, M. R. and Clattenburg, R. E. (1985). Ependyma: normal and pathological. A review of the literature. *Brain Res.* **356**, 1-19.

Bush, A. (2000). Primary ciliary dyskinesia. *Acta Otorhinolaryngol. Belg.* **54**, 317-324.

Cano, D. A., Murcia, N. S., Pazour, G. J. and Hebrok, M. (2004). Orpk mouse model of polycystic kidney disease reveals essential role of primary cilia in pancreatic tissue organization. *Development* **131**, 3457-3467.

Chen, J., Knowles, H. J., Hebert, J. L. and Hackett, B. P. (1998). Mutation of the mouse hepatocyte nuclear factor/forkhead homologue 4 gene results in an absence of cilia and random left-right asymmetry. *J. Clin. Invest.* **102**, 1077-1082.

Davy, B. E. and Robinson, M. L. (2003). Congenital hydrocephalus in hy3 mice is caused by a frameshift mutation in Hydin, a large novel gene. *Hum. Mol. Genet.* **12**, 1163-1170.

DeMattos, R. B., Bales, K. R., Parsadanian, M., O'Dell, M. A., Foss, E. M., Paul, S. M. and Holtzman, D. M. (2002). Plaque-associated disruption of CSF and plasma amyloid-beta (Abeta) equilibrium in a mouse model of Alzheimer's disease. *J. Neurochem.* **81**, 229-236.

Doolin, P. F. and Birge, W. J. (1966). Ultrastructural organization of cilia and basal bodies of the epithelium of the choroid plexus in the chick embryo. *J. Cell Biol.* **29**, 333-345.

Garton, H. J. and Piatt, J. H., Jr (2004). Hydrocephalus. *Pediatr. Clin. North Am.* **51**, 305-325.

Guay-Woodford, L. M. (2003). Murine models of polycystic kidney disease: molecular and therapeutic insights. *Am. J. Physiol. Renal Physiol.* **285**, F1034-F1049.

Haycraft, C. J., Swoboda, P., Taulman, P. D., Thomas, J. H. and Yoder, B. K. (2001). The C. elegans homolog of the murine cystic kidney disease gene Tg737 functions in a ciliogenic pathway and is disrupted in osm-5 mutant worms. *Development* **128**, 1493-1505.

Ibanez-Tallon, I., Pagenstecher, A., Fliegauf, M., Olbrich, H., Kispert, A., Ketelsen, U. P., North, A., Heintz, N. and Omran, H. (2004). Dysfunction of axonemal dynein heavy chain Mdnah5 inhibits ependymal flow and reveals a novel mechanism for hydrocephalus formation. *Hum. Mol. Genet.* **13**, 2133-2141.

Ibraghimov-Beskrovnaya, O., Dackowski, W. R., Foggensteiner, L., Coleman, N., Thiru, S., Petry, L. R., Burn, T. C., Connors, T. D., Van Raay, T. et al. (1997). Polycystin: in vitro synthesis, in vivo tissue expression, and subcellular localization identifies a large membrane-associated protein. *Proc. Natl. Acad. Sci. USA* **94**, 6397-6402.

Jones, H. C. and Bucknall, R. M. (1988). Inherited prenatal hydrocephalus in the H-Tx rat: a morphological study. *Neuropathol. Appl. Neurobiol.* **14**, 263-274.

Kibble, J. D., Garner, C., Colledge, W. H., Brown, S., Kajita, H., Evans, M. and Brown, P. D. (1997). Whole cell Cl- conductances in mouse choroid plexus epithelial cells do not require CFTR expression. *Am. J. Physiol.* **272**, C1899-C1907.

Kiefer, M., Eymann, R., von Tiling, S., Muller, A., Steudel, W. I. and Booz, K. H. (1998). The ependyma in chronic hydrocephalus. *Childs Nerv. Syst.* **14**, 263-270.

Lindeman, G. J., Dagnino, L., Gaubatz, S., Xu, Y., Bronson, R. T., Warren, H. B. and Livingston, D. M. (1998). A specific, nonproliferative role for E2F-5 in choroid plexus function revealed by gene targeting. *Genes Dev.* **12**, 1092-1098.

Liu, W., Murcia, N. S., Duan, Y., Weinbaum, S., Yoder, B. K., Schwiebert, E. and Satlin, L. M. (2005). Mechanoregulation of intracellular Ca2+ concentration is attenuated in collecting duct of monocilium-impaired orpk mice. *Am. J. Physiol. Renal Physiol*. **289**, F978-F988.

Moyer, J. H., Lee-Tischler, M. J., Kwon, H. Y., Schrick, J. J., Avner, E. D., Sweeney, W. E., Godfrey, V. L., Cacheiro, N. L., Wilkinson, J. E. and Woychik, R. P. (1994). Candidate gene associated with a mutation causing recessive polycystic kidney disease in mice. *Science* **264**, 1329-1333.

Nauli, S. M., Alenghat, F. J., Luo, Y., Williams, E., Vassilev, P., Li, X., Elia, A. E., Lu, W., Brown, E. M., Quinn, S. J. et al. (2003). Polycystins 1 and 2 mediate mechanosensation in the primary cilium of kidney cells. *Nat. Genet.* **33**, 129-137.

Olteanu, D., Yoder, B. K., Liu, W., Croyle, M. J., Welty, E. A., Rosborough, K., Wyss, J. M., Bell, P. D., Guay-Woodford, L. M., Bevensee, M. O. et al. (2005). Heightened ENaC-mediated sodium absorption in a murine polycystic kidney diease model epithelium lacking apical monocilia. *Am. J. Physiol. Cell Physiol.* (in press).

Pazour, G. J., Dickert, B. L., Vucica, Y., Seeley, E. S., Rosenbaum, J. L., Witman, G. B. and Cole, D. G. (2000). Chlamydomonas IFT88 and its mouse homologue, polycystic kidney disease gene tg737, are required for assembly of cilia and flagella. *J. Cell Biol.* **151**, 709-718.

Praetorius, H. A. and Spring, K. R. (2003). The renal cell primary cilium functions as a flow sensor. *Curr. Opin. Nephrol. Hypertens.* **12**, 517-520.

Rolf, B., Kutsche, M. and Bartsch, U. (2001). Severe hydrocephalus in L1-deficient mice. *Brain Res.* **891**, 247-252.

Ruiz, A., Sklar, E. M. L. and Quencer, R. M. (2004). Structural Neuroimaging. In *Neurology in Clinical Practice* (ed. W. G. Bradley, R. B. Daroff, G. M. Fenichel and C. D. Marsden), pp. 521-595. Woburn, MA: Butterworth-Heinemann.

Sapiro, R., Kostetskii, I., Olds-Clarke, P., Gerton, G. L., Radice, G. L. and Strauss III, J. F. (2002). Male infertility, impaired sperm motility, and hydrocephalus in mice deficient in sperm-associated antigen 6. *Mol. Cell. Biol.* **22**, 6298-6305.

Scholey, J. M. (2003). Intraflagellar transport. *Annu. Rev. Cell Dev. Biol.* **19**, 423-443.

Strazielle, N. and Ghersi-Egea, J. F. (2000). Choroid plexus in the central nervous system: biology and physiopathology. *J. Neuropathol. Exp. Neurol.* **59**, 561-574.

Sullivan, L. P., Wallace, D. P. and Grantham, J. J. (1998). Epithelial transport in polycystic kidney disease. *Physiol. Rev.* **78**, 1165-1191.

Sutters, M. and Germino, G. G. (2003). Autosomal dominant polycystic kidney disease: molecular genetics and pathophysiology. *J. Lab. Clin. Med.* **141**, 91-101.

Taulman, P. D., Haycraft, C. J., Balkovetz, D. F. and Yoder, B. K. (2001). Polaris, a protein involved in left-right axis patterning, localizes to basal bodies and cilia. *Mol. Biol. Cell* **12**, 589-599.

Torikata, C., Kijimoto, C. and Koto, M. (1991). Ultrastructure of respiratory cilia of WIC-Hyd male rats. An animal model for human immotile cilia syndrome. *Am. J. Pathol.* **138**, 341-347.

Torres, V. E. (2004). Therapies to slow polycystic kidney disease. *Nephron Exp. Nephrol.* **98**, E1-E7.

Weller, R. O., Kida, S. and Zhang, E. T. (1992). Pathways of fluid drainage from the brain – morphological aspects and immunological significance in rat and man. *Brain Pathol.* **2**, 277-284.

Wilson, P. D. (1997). Epithelial cell polarity and disease. *Am. J. Physiol.* **272**, F434-F442.

Yoder, B. K., Richards, W. G., Sommardahl, C., Sweeney, W. E., Michaud, E. J., Wilkinson, J. E., Avner, E. D. and Woychik, R. P. (1997). Differential rescue of the renal and hepatic disease in an autosomal recessive

polycystic kidney disease mouse mutant. A new model to study the liver lesion. *Am. J. Pathol.* **150**, 2231-2241.

Yoder, B. K., Tousson, A., Millican, L., Wu, J. H., Bugg, C. E., Jr, Schafer, J. A. and Balkovetz, D. F. (2002). Polaris, a protein disrupted in orpk mutant mice, is required for assembly of renal cilium. *Am. J. Physiol. Renal Physiol.* **282**, F541-F552.

Zhang, Q., Murcia, N. S., Chittenden, L. R., Richards, W. G., Michaud, E. J., Woychik, R. P. and Yoder, B. K. (2003). Loss of the Tg737 protein results in skeletal patterning defects. *Dev. Dyn.* **227**, 78-90.

Zhang, Q., Davenport, J. R., Croyle, M. J., Haycraft, C. J. and Yoder, B. K. (2005). Disruption of IFT results in both exocrine and endocrine abnormalities in the pancreas of Tg737(orpk) mutant mice. *Lab. Invest.* **85**, 45-64.